PTEP

Prog. Theor. Exp. Phys. **2020**, 063D03 (17 pages)
DOI: 10.1093/ptep/ptaa070

Feasibility study of the $K^+d \to K^0pp$ reaction for the Θ^+ pentaquark

Takayasu Sekihara[1,2,3,*], Hyun-Chul Kim[1,4,5], and Atsushi Hosaka[1,2]

[1]*Advanced Science Research Center, Japan Atomic Energy Agency, Shirakata, Tokai, Ibaraki 319-1195, Japan*
[2]*Research Center for Nuclear Physics (RCNP), Osaka University, Ibaraki, Osaka 567-0047, Japan*
[3]*RIKEN, Wako, Saitama 351-0198, Japan*
[4]*Department of Physics, Inha University, Incheon 22212, Republic of Korea*
[5]*School of Physics, Korea Institute for Advanced Study (KIAS), Seoul 02455, Republic of Korea*
[*]E-mail: sekihara@post.j-parc.jp

Received October 22, 2019; Revised April 5, 2020; Accepted April 19, 2020; Published June 24, 2020

We investigate theoretically the K^0p invariant mass spectrum of the $K^+d \to K^0pp$ reaction and scrutinize how the signal of the "Θ^+" pentaquark, if it exists, emerges in the K^0p spectrum. The most prominent advantage of this reaction is that we can clearly assess whether the "Θ^+" exists or not as a direct-formation production without significant backgrounds, in contrast to other reactions such as photoproduction and π-induced productions. We show that while the impulse or single-step scattering process can cover the "Θ^+" energy region with an initial kaon momentum $k_{\rm lab} \approx 0.40$ GeV/c in the laboratory frame, the contributions from double-step processes may have a potential possibility to reach the "Θ^+" energy region with a higher kaon momentum $k_{\rm lab} \sim 1$ GeV/c. Assuming that the full decay width of the "Θ^+" is around 0.5 MeV, we predict that the magnitude of the peak corresponding to the "Θ^+" is around a few hundred μb to 1 mb with the momentum of the kaon beam $k_{\rm lab} \approx 0.40$ GeV/c while it is around $\lesssim 1$ μb with $k_{\rm lab} \approx 0.85$ GeV/c. Thus, the "Θ^+" peak is more likely to be seen at $k_{\rm lab} \approx 0.40$ GeV/c than at $k_{\rm lab} \approx 0.85$ GeV/c.

Subject Index D32

1. Introduction

The physics of pentaquarks, which are baryons consisting of four valence quarks and one antiquark, has been renewed very recently, as the LHCb Collaboration announced new findings of three heavy pentaquarks, P_c [1–4]. The LHCb Collaboration also found five excited Ω_c in the channel of the $\Xi_c^+K^-$ invariant mass [5]. Four of them were confirmed by the Belle Collaboration [6]. Since these newly found excited Ω_c have very small decay widths, several theoretical works have suggested that at least some of them may be identified as singly heavy pentaquarks [7–10]. On the other hand, discussion of light pentaquarks, which was once triggered by the theoretical prediction [11] and the first measurement of the Θ^+ [12], has become dormant since the null results of the Θ^+ baryon were reported by the CLAS Collaboration [13–15]. Moreover, both the KEK-PS E533 Collaboration [16] and the J-PARC E19 Collaboration [17,18] searched for the "Θ^+" using the pion beam but found no significant peak corresponding to the "Θ^+" pentaquark. The Belle Collaboration looked for isospin partners of the "Θ^+" in the first observed process $\gamma\gamma \to p\bar{p}K^+K^-$ but again found no significant evidence for them [19]. All these negative results make the existence of the "Θ^+" rather unlikely, so that both experimental and theoretical investigations on the "Θ^+" ebbed away.

Funded by SCOAP[3]

Meanwhile, the LEPS Collaboration and DIANA Collaboration continued to report evidence for the existence of the "Θ^+" [20–23]. Some years ago, Amaryan et al. analyzed the data from the CLAS Collaboration [24], using the interference method with ϕ-meson photoproduction. They found a peak around $\sim$ 1.54 GeV, which corresponds to the "Θ^+". The statistical significance of this peak was 5.3σ [24]. In Ref. [25], the SELEX data on hadro-nucleus collisions at Fermilab were analyzed in the search for formation of the "Θ^+". A narrow enhancement near 1539 MeV was observed in the mass spectrum of the pK_S^0 system emitted at small x_F from hadron collisions with copper nuclei, where x_F denotes the Feynman variable defined as the ratio of the momentum $p_L^*/p_{\rm max}^*$ (for details see Ref. [25]). However, the results from Ref. [25] show definite dependence on the kinematics.

After the LHCb Collaboration reported the existence of heavy pentaquarks, interest in light pentaquarks seems to have been renewed. For example, the existence of a narrow nucleon resonance $N^*(1685)$ has been announced by a series of experiments in η photoproduction off the quasi-neutron [26–35]. More recently, a similar narrow peak was observed in the $\gamma p \to p\pi^0\eta$ reaction [36]. Though the identification of this narrow resonance is still under debate, one possible interpretation is that it can be regarded as a pentaquark nucleon, which is a member of the baryon antidecuplet [37–39].

Based on previous experimental studies on the "Θ^+", we could draw at least one conclusion: the "Θ^+" is most unlikely to exist. Even though it might exist, it is elusive. However, we want to mention that almost all previous experiments have utilized indirect methods such as photon and pion beams, which suffer from large backgrounds [40,41]. Moreover, we know that the "Θ^+", if it exists, decays into K^0p or K^+n and hence couples to them. In particular, the K^+n channel may be the most probable one to search for the "Θ^+". In fact, the DIANA Collaboration used the low-energy K^+Xe reaction in the xenon bubble chamber [22,23,42–44], though there is also a theoretical criticism of the DIANA results in 2003 [45]. Nevertheless, the K^+ beam may provide an ultimate smoking gun to whether the "Θ^+" exists or not, since it will create the "Θ^+" by direct formation and it will be seen in the differential and total cross sections if it exists. There is also a discussion on K^+N reactions in a nucleus [46]. Thus, measuring the $K^+d \to K^0pp$ reaction is the simplest and final experiment to put a period to the existence of the "Θ^+" pentaquark. This process, compared with other reactions such as photoproduction and π-induced productions, is not hampered by significant backgrounds. This means that the experiment of $K^+d \to K^0pp$ will clearly assess the existence of the "Θ^+".

The $K^+d \to K^0pp$ reaction has already been investigated theoretically [47] with the width of the "Θ^+" being assumed to be 1–20 MeV. Simulations were also performed for experiments proposed at J-PARC [48,49]. In Ref. [47] Sibirtsev et al. considered the single-step process or the impulse scattering process in which the proton in the deuteron was regarded as a spectator and the neutron interacts with the K^+ to produce a proton and a neutral kaon. When the K^+ momentum lies in the range of 0.47–0.64 GeV/c, the peak corresponding to the "Θ^+" was seen in the K^0p invariant mass spectra. In the vicinity of 0.47 GeV/c, the "Θ^+" peak was also shown in the total cross sections. In the present work, we include both the single-step and double-step processes and scrutinize the feasibility of the $K^+d \to K^0pp$ reaction in observing the "Θ^+" pentaquark. The use of the double-step process was also proposed in Ref. [50]. In the double-step processes, a kaon is exchanged in the course of the interaction between the proton and the neutron. We will show that in the present work the single-step process can cover the energy region corresponding to the "Θ^+" peak with an initial kaon momentum $k_{\rm lab} \approx 0.4$ GeV/c in the laboratory frame while the double-step processes provide a potential possibility to reach the "Θ^+" energy region with a higher kaon momentum $k_{\rm lab} \approx 1$ GeV/c. In the present work, therefore, we will carefully investigate the $K^+d \to K^0pp$ reaction in the context of the possible existence of the "Θ^+", considering both the single- and double-step processes.

This paper is organized as follows. In Sect. 2, we formulate the cross section of the $K^+d \to K^0pp$ reaction. The $KN \to KN$ scattering amplitude is also shown in this section. In Sect. 3, we give numerical results on the cross section of the $K^+d \to K^0pp$ reaction and investigate the strength of a peak signal in the K^0p spectrum, which will provide a good guideline to conclude whether the "Θ^+" exists or not. Section 4 is devoted to the summary of this study.

2. Formulation

2.1. Cross section of the $K^+d \to K^0pp$ reaction

First of all, we formulate the cross section of the $K^+d \to K^0pp$ reaction. Since we are interested in the K^0p invariant mass spectrum, in which we search for the "Θ^+" signal, it is convenient to calculate the differential cross section as a function of the K^0p invariant mass together with the scattering angle for the other proton. In this respect, we can express the differential cross section of this reaction as [51–54]

$$\frac{d^2\sigma}{dM_{K^0p}d\cos\theta_2'} = \frac{m_d m_p^2}{64\pi^4 k_{\rm cm} W^2} p_2' p_K^* \int d\Omega_K^* |\mathcal{T}|^2. \tag{1}$$

Before we explain Eq. (1), let us distinguish the two protons in the final state. We will call the proton that is involved in producing the "Θ^+" together with K^0 the "first" proton, whereas the other one is called the "second" proton. M_{K^0p} in Eq. (1) denotes the invariant mass of the K^0 and "first" p, θ_2' stands for the scattering angle for the "second" proton in the center-of-mass (CM) frame of the K^+d system, and Ω_K^* represents the solid angle for the K^0 in the rest frame of the K^0 and first p. W is the CM energy of the K^+d system, and m_d and m_p correspond to the masses of the deuteron and proton, respectively. The prefactor of the cross section contains the following momenta: the initial kaon momentum $k_{\rm cm}$ and the final second proton momentum p_2' are evaluated within the CM frame, while the final kaon momentum p_K^* is obtained in the rest frame of the K^0 and first p. They are calculated as

$$k_{\rm cm} = \frac{\lambda^{1/2}(W^2, m_{K^+}^2, m_d^2)}{2W}, \quad p_2' = \frac{\lambda^{1/2}(W^2, M_{K^0p}^2, m_p^2)}{2W}, \quad p_K^* = \frac{\lambda^{1/2}(M_{K^0p}^2, m_{K^0}^2, m_p^2)}{2M_{K^0p}}, \tag{2}$$

where $\lambda(x, y, z) \equiv x^2 + y^2 + z^2 - 2xy - 2yz - 2zx$. $|\mathcal{T}|^2$ denotes the squared scattering amplitude.

When we calculate the K^0p invariant mass spectrum or total cross section, we need a factor $1/2$ to avoid double counting of the two protons in the final state:

$$\frac{d\sigma}{dM_{K^0p}} = \frac{1}{2}\int \cos\theta_2' \frac{d^2\sigma}{dM_{K^0p}d\cos\theta_2'}, \quad \sigma = \frac{1}{2}\int dM_{K^0p}\int \cos\theta_2' \frac{d^2\sigma}{dM_{K^0p}d\cos\theta_2'}. \tag{3}$$

In addition to the differential cross section $d^2\sigma/dM_{K^0p}d\cos\theta_2'$, we may consider $d^2\sigma/dM_{K^0p(1)}dM_{K^0p(2)}$ as a Dalitz plot of the $K^+d \to K^0pp$ reaction, where $M_{K^0p(1)}$ ($M_{K^0p(2)}$) is the invariant mass of the K^0 and "first" ("second") proton. We can calculate this by the formula

$$\frac{d^2\sigma}{dM_{K^0p(1)}dM_{K^0p(2)}} = \frac{m_d m_p^2}{128\pi^4 k_{\rm cm} W^3} M_{K^0p(1)} M_{K^0p(2)} \int d\cos\theta_2' \int d\phi_K^* |\mathcal{T}|^2, \tag{4}$$

where ϕ_K^* is the azimuthal angle for the K^0 in the rest frame of the K^0 and first p.

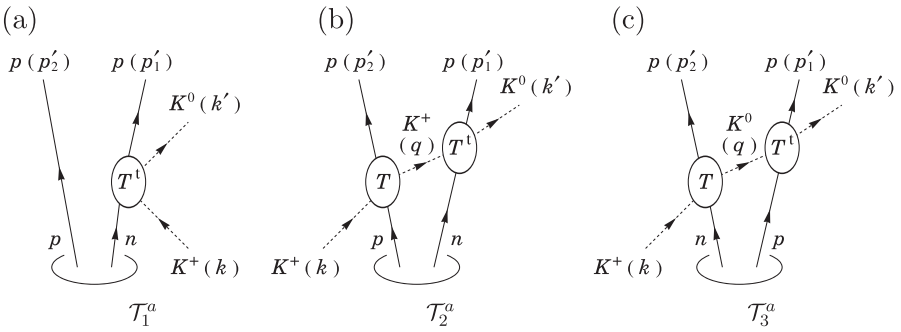

Fig. 1. Diagrams for the $K^+d \to K^0pp$ reaction. Momenta of particles are shown in parentheses.

2.2. Scattering amplitude of the $K^+d \to K^0pp$ reaction

Next we construct the scattering amplitude of the $K^+d \to K^0pp$ reaction. Since the deuteron has spin 1, the scattering amplitude can be denoted by $\mathcal{T}^a$ with $a = 1,\ 2$, and 3 to specify the deuteron spin component. As depicted in Fig. 1 together with the momenta of particles, the reaction mechanism consists of the three main diagrams: $\mathcal{T}_1^a$ stands for the impulse scattering process [47], and $\mathcal{T}_2^a$ and $\mathcal{T}_3^a$ represent the double-step scattering processes, where the intermediate kaons K^+ and K^0 propagate respectively between two nucleons[1]. Thus, the $K^+d \to K^0pp$ scattering amplitude is expressed as the sum of these three contributions:

$$\begin{aligned}\mathcal{T}^a =& \mathcal{T}_1^a(k^\mu, k'^\mu, p_1'^\mu, p_2'^\mu) + \mathcal{T}_2^a(k^\mu, k'^\mu, p_1'^\mu, p_2'^\mu) + \mathcal{T}_3^a(k^\mu, k'^\mu, p_1'^\mu, p_2'^\mu) \\ & - (\text{antisymmetric terms}),\end{aligned} \tag{5}$$

where the antisymmetric terms are required owing to the identical fermions, i.e., protons in the final state. We now derive the K^+d scattering amplitude in the laboratory frame, in which the deuteron three-momentum satisfies $\boldsymbol{p}_d = \boldsymbol{0}$. In particular, we evaluate each $KN \to KN$ amplitude in the target-baryon rest frame, as we will show below.

The impulse scattering amplitude $\mathcal{T}_1^a$, depicted in Fig. 1(a), is calculated as [54]

$$\mathcal{T}_1^a(k^\mu, k'^\mu, p_1'^\mu, p_2'^\mu) = \tilde{\varphi}(|\boldsymbol{p}_2'|)(S^\dagger)^a T^{\rm t}_{K^+n\to K^0p}(w_1; \boldsymbol{k}, \boldsymbol{k}'). \tag{6}$$

Here, $T_{K^+n\to K^0p}$ stands for the $K^+n \to K^0p$ scattering amplitude in a 2×2 matrix form, which is represented in the spin space of the nucleon, and the superscript t designates the transpose of a 2×2 matrix. The $K^+n \to K^0p$ amplitude depends on the CM energy $w_1 = \sqrt{(k'^\mu + p_1'^\mu)^2}$ and three-momenta of the initial and final kaons in the laboratory frame, $\boldsymbol{k}$ and $\boldsymbol{k}'$, respectively. The deuteron spin component is denoted by $(S^\dagger)^a = -i\sigma^2\sigma^a/\sqrt{2}$ $(a = 1, 2, 3)$ in a 2×2 matrix form with the Pauli matrices σ^a. $\tilde{\varphi}$ is the deuteron wave function in momentum space, for which we neglect the d-wave component because it is negligibly small. An analytic parametrization of the s-wave component [56] facilitates the handling of the deutron wave function in an easy manner:

$$\tilde{\varphi}(p) = \sum_{j=1}^{11} \frac{C_j}{p^2 + m_j^2}, \tag{7}$$

[1] The double scattering contributions in the K^+d reaction were taken into account in, e.g., Ref. [55] but in the case of lower kaon momenta.

with C_j and m_j determined in Ref. [57]. As we mentioned previously, each part of the K^+d scattering amplitude, i.e., the deuteron wave function and the $K^+n \to K^0p$ amplitude, is evaluated in the laboratory frame. The expression for the $K^+n \to K^0p$ amplitude in the target-baryon rest frame will be given in Sect. 2.3.

The double-step scattering amplitudes, $\mathcal{T}_2^a$ and $\mathcal{T}_3^a$, which are depicted respectively in Figs. 1(b) and (c), are calculated as [54]

$$\mathcal{T}_2^a(k^\mu, k'^\mu, p_1'^\mu, p_2'^\mu) = \int \frac{d^3q}{(2\pi)^3} \frac{\tilde{\varphi}(|\boldsymbol{q}+\boldsymbol{p}_2'-\boldsymbol{k}|)}{(q^0)^2-\boldsymbol{q}^2-m_{K^+}^2+i0} F(|\boldsymbol{q}|) \times T_{K^+p\to K^+p}(w_2; \boldsymbol{k}, \boldsymbol{q})(S^\dagger)^a T^{\mathrm{t}}_{K^+n\to K^0p}(w_1; \boldsymbol{q}, \boldsymbol{k}'), \tag{8}$$

$$\mathcal{T}_3^a(k^\mu, k'^\mu, p_1'^\mu, p_2'^\mu) = -\int \frac{d^3q}{(2\pi)^3} \frac{\tilde{\varphi}(|\boldsymbol{q}+\boldsymbol{p}_2'-\boldsymbol{k}|)}{(q^0)^2-\boldsymbol{q}^2-m_{K^0}^2+i0} F(|\boldsymbol{q}|) \times T_{K^+n\to K^0p}(w_2; \boldsymbol{k}, \boldsymbol{q})(S^\dagger)^a T^{\mathrm{t}}_{K^0p\to K^0p}(w_1; \boldsymbol{q}, \boldsymbol{k}'), \tag{9}$$

where $F(q)$ represents a form factor for which we take a Gaussian form of $F(q) = \exp(-q^2/\Lambda^2)$ with a cutoff Λ. The kaon energies in the propagators are fixed in the truncated Faddeev approach [53] as

$$q^0 = k^0 + m_d - p_2'^0 - \sqrt{|\boldsymbol{q}+\boldsymbol{p}_2'-\boldsymbol{k}|^2+m_N^2}, \tag{10}$$

where the energy–momenta of the particles are fixed in the laboratory frame and m_N is the isospin-averaged nucleon mass $m_N = (m_p + m_n)/2$. The CM energy for the first collision is given by $w_2 = \sqrt{(q^\mu + p_2'^\mu)^2}$, and hence it depends on the Fermi motion of bound nucleons as well as on the initial kaon momentum.

As for the antisymmetric terms, we have to calculate the scattering amplitudes where the momenta and spins of the two protons are simultaneously exchanged, i.e., $(p_1^\mu, s_1) \leftrightarrow (p_2^\mu, s_2)$ with $s_{1,2}$ being the spins of protons. This antisymmetrization for the present scattering amplitudes can be performed in the following manner:

$$\left[\mathcal{T}^a_{1,2,3}(k^\mu, k'^\mu, p_1'^\mu, p_2'^\mu)\right]_{\text{antisymmetric}} = \mathcal{T}^a_{1,2,3}{}^{\mathrm{t}}(k^\mu, k'^\mu, p_2'^\mu, p_1'^\mu). \tag{11}$$

Finally, the squared scattering amplitude in Eq. (1) is obtained by the spin average and summation for the initial deuteron and final protons, respectively, which results in the following expression [54]:

$$|\mathcal{T}|^2 = \frac{1}{3}\sum_{a=1}^{3} \mathrm{tr}\left[\mathcal{T}^a\left(\mathcal{T}^a\right)^\dagger\right]. \tag{12}$$

2.3. Scattering amplitude of the KN → KN reaction

We turn to the $KN \to KN$ scattering amplitude $T_{KN\to KN}$, which is expressed in terms of a 2×2 matrix. In the present work, we first present the $KN \to KN$ amplitude in terms of the partial waves in the CM frame of the KN system, and then transform it to that in the target-baryon rest frame, taking the method in Ref. [58].

The KN amplitude is generally expressed in the KN CM frame as:

$$T^{\rm cm}_{KN\to KN}(w;\boldsymbol{p}^*_{\rm in},\boldsymbol{p}^*_{\rm out}) = g^{\rm cm}_{KN\to KN}(w,p^*_{\rm in},p^*_{\rm out},x^*) - ih^{\rm cm}_{KN\to KN}(w,p^*_{\rm in},p^*_{\rm out},x^*)\frac{(\boldsymbol{p}^*_{\rm out}\times\boldsymbol{p}^*_{\rm in})\cdot\boldsymbol{\sigma}}{p^*_{\rm out}p^*_{\rm in}}, \tag{13}$$

where w denotes the CM energy and $\boldsymbol{p}^*_{\rm in}$ ($\boldsymbol{p}^*_{\rm out}$) stands for the three-momentum for the initial (final) kaon in the CM frame. Then, we can define $p^*_{\rm out,in}\equiv|\boldsymbol{p}^*_{\rm out,in}|$ and $x^*\equiv\boldsymbol{p}^*_{\rm out}\cdot\boldsymbol{p}^*_{\rm in}/(p^*_{\rm out}p^*_{\rm in})$. The Pauli matrices $\boldsymbol{\sigma}$ act on the nucleon spinors, and $g^{\rm cm}_{KN\to KN}$ and $h^{\rm cm}_{KN\to KN}$ are expressed in terms of the partial waves as

$$g^{\rm cm}_{KN\to KN}(w,p^*_{\rm in},p^*_{\rm out},x^*) = \sum_{L=0}^{\infty}\left[(L+1)T^{\rm cm}_{KN\to KN,L+}(w,p^*_{\rm in},p^*_{\rm out}) + LT^{\rm cm}_{KN\to KN,L-}(w,p^*_{\rm in},p^*_{\rm out})\right]P_L(x^*), \tag{14}$$

$$h^{\rm cm}_{KN\to KN}(w,p^*_{\rm in},p^*_{\rm out},x^*) = \sum_{L=1}^{\infty}\left[T^{\rm cm}_{KN\to KN,L+}(w,p^*_{\rm in},p^*_{\rm out}) - T^{\rm cm}_{KN\to KN,L-}(w,p^*_{\rm in},p^*_{\rm out})\right]P'_L(x^*), \tag{15}$$

with the Legendre polynomials $P_L(x)$, $P'_L(x)\equiv dP_L/dx$, and orbital angular momentum L.

Next we transform the above-given amplitudes to that in the target-baryon rest frame according to the formula [58]

$$T_{KN\to KN}(w;\boldsymbol{p}_{\rm in},\boldsymbol{p}_{\rm out}) = \sqrt{\frac{\omega_K(p^*_{\rm in})E_N(p^*_{\rm in})\omega_K(p^*_{\rm out})E_N(p^*_{\rm out})}{\omega_K(p_{\rm in})m_N\omega_K(p_{\rm out})E_N(|\boldsymbol{p}_{\rm in}-\boldsymbol{p}_{\rm out}|)}}T^{\rm cm}_{KN\to KN}(w;\boldsymbol{p}^*_{\rm in},\boldsymbol{p}^*_{\rm out}) \tag{16}$$

where parameters in the target-baryon rest frame are expressed without asterisks in contrast to those in the CM frame. The Lorentz-boost factor appears in the right-hand side and contains the kaon energy $\omega_K(p)\equiv\sqrt{m_K^2+p^2}$ with the isospin-averaged kaon mass $m_K=(m_{K^+}+m_{K^0})/2$ and nucleon energy $E_N(p)\equiv\sqrt{m_N^2+p^2}$.

We now construct the partial-wave amplitudes $T^{\rm cm}_{KN\to KN,L\pm}$, which should be in general off-shell amplitudes and thus functions of three independent variables: w, $p^*_{\rm in}$, and $p^*_{\rm out}$. In the present study, we assume that the partial-wave amplitudes depend on the momenta minimally required by the kinematics; i.e., the off-shell amplitudes are proportional to $(p^*_{\rm out}p^*_{\rm in})^L$. Under this assumption, we have an advantage that the on-shell amplitudes can simulate the off-shell amplitudes by introducing the formula

$$T^{\rm cm}_{KN\to KN,L\pm}(w,p^*_{\rm out},p^*_{\rm in}) = T^{\text{on-shell}}_{KN\to KN,L\pm}(w)\frac{(p^*_{\rm out}p^*_{\rm in})^L}{[p^{\text{on-shell}}(w)]^{2L}}, \tag{17}$$

where $p^{\text{on-shell}}$ is the on-shell momentum for the KN system:

$$p^{\text{on-shell}}(w) = \frac{\lambda^{1/2}(w^2,m_K^2,m_N^2)}{2w}. \tag{18}$$

Since we need the KN amplitudes in the energy range from its threshold to $w \sim 2$ GeV, we utilize the on-shell KN amplitude developed in the SAID program [59], in which they provide the on-shell KN amplitude in various partial waves. We here take the SAID partial-wave amplitudes up to the D waves and calculate the off-shell amplitudes by using Eq. (17).

Finally we introduce the "Θ^+" contribution, which is just added as an s-channel "Θ^+" exchange term to the KN scattering amplitude in the present study. Here we assume the "Θ^+" to be an isosinglet, and examine four different cases of its spin/parity $J^P = 1/2^\pm$ and $3/2^\pm$. The KN"Θ" coupling is governed by an effective Lagrangian as follows:

$$\mathcal{L} = g_{KN\Theta}\overline{\Theta}\Gamma(K^+ n - K^0 p) + \text{h.c.}, \tag{19}$$

in the spin $1/2$ case, where $\Gamma = 1$ $(i\gamma_5)$ for the negative (positive) parity and $g_{KN\Theta}$ denotes the coupling constant, and

$$\mathcal{L} = \frac{-ig_{KN\Theta}}{m_K}\overline{\Theta}^\mu \gamma_5 \Gamma(\partial_\mu K^+ n - \partial_\mu K^0 p) + \text{h.c.}, \tag{20}$$

in the spin $3/2$ case. This provides us with the formula for the "Θ^+" decay width:

$$\Gamma_{\Theta\to K^+n} = \Gamma_{\Theta\to K^0 p} = \begin{cases} \dfrac{g_{KN\Theta}^2 p_K^* \left(E_N(p_K^*) \mp m_N\right)}{4\pi M_\Theta} & \text{for } J^P = 1/2^\pm, \\ \dfrac{g_{KN\Theta}^2 p_K^{*3} \left(E_N(p_K^*) \pm m_N\right)}{12\pi m_K^2 M_\Theta} & \text{for } J^P = 3/2^\pm, \end{cases} \tag{21}$$

where M_Θ stands for the "Θ^+" mass and p_K^* designates the CM momentum of the final-state KN system. Thus, using the "Θ^+" mass M_Θ and full decay width $\Gamma_\Theta = \Gamma_{\Theta\to K^+n} + \Gamma_{\Theta\to K^0 p}$, we can fix the coupling constant $g_{KN\Theta}$. In the present study we use a presumed value of the mass $M_\Theta = 1524$ MeV [20] and a predicted value of the decay width $\Gamma_\Theta = 0.5$ MeV [60], which results in $g_{KN\Theta} = 0.783$ for $J^P = 1/2^+$, $g_{KN\Theta} = 0.101$ for $1/2^-$, $g_{KN\Theta} = 0.352$ for $3/2^+$, and $g_{KN\Theta} = 2.734$ for $3/2^-$. Then, the s-channel "Θ^+" exchange term enters into the partial-wave $K^+n \to K^+n$ amplitude as

$$T^{(\Theta)}_{K^+n\to K^+n,\,1-}(w; p_{\text{in}}^*, p_{\text{out}}^*) = \frac{p_{\text{out}}^* p_{\text{in}}^*}{4m_N^2} \frac{g_{KN\Theta}^2}{w - M_\Theta + i\Gamma_\Theta/2} \qquad \text{for } J^P = 1/2^+, \tag{22}$$

$$T^{(\Theta)}_{K^+n\to K^+n,\,0+}(w; p_{\text{in}}^*, p_{\text{out}}^*) = \frac{g_{KN\Theta}^2}{w - M_\Theta + i\Gamma_\Theta/2} \qquad \text{for } J^P = 1/2^-, \tag{23}$$

$$T^{(\Theta)}_{K^+n\to K^+n,\,1+}(w; p_{\text{in}}^*, p_{\text{out}}^*) = \frac{p_{\text{out}}^* p_{\text{in}}^*}{3m_K^2} \frac{g_{KN\Theta}^2}{w - M_\Theta + i\Gamma_\Theta/2} \qquad \text{for } J^P = 3/2^+, \tag{24}$$

$$T^{(\Theta)}_{K^+n\to K^+n,\,2-}(w; p_{\text{in}}^*, p_{\text{out}}^*) = \frac{(p_{\text{out}}^* p_{\text{in}}^*)^2}{12m_K^2 m_N^2} \frac{g_{KN\Theta}^2}{w - M_\Theta + i\Gamma_\Theta/2} \qquad \text{for } J^P = 3/2^-. \tag{25}$$

The "Θ^+" contributions to the $K^+n \to K^0p$ and $K^0p \to K^0p$ amplitudes are evaluated with the isospin relation $T^{(\Theta)}_{K^+n\to K^0p} = -T^{(\Theta)}_{K^0p\to K^0p} = -T^{(\Theta)}_{K^+n\to K^+n}$.

3. Numerical results and discussion

We are now in a position to present the numerical results and discuss their physical implications, in particular how the signal of the "Θ^+" pentaquark, if it exists, emerges in the K^0p spectrum.

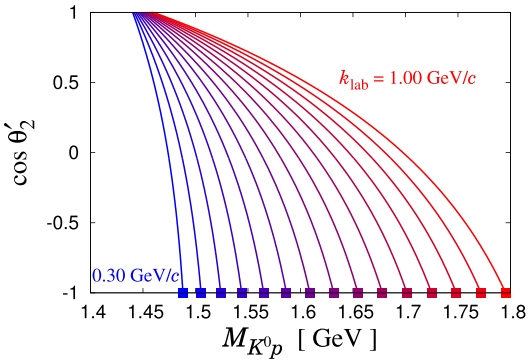

Fig. 2. Possible K^0p invariant mass of the $K^+d \to K^0pp$ reaction with the impulse scattering process as a function of the scattering angle for the "second" proton in the global CM frame θ_2'. The initial kaon momentum in the laboratory frame $k_{\rm lab}$ is taken from 0.30 GeV/c to 1.00 GeV/c in intervals of 0.05 GeV/c. We assume zero Fermi motion. The square boxes represent the invariant mass of K^0 and the proton produced in the impulse process, while the lines represent that of K^0 and the spectator proton.

3.1. Two mechanisms to reach the "Θ^+" energy

Before we discuss the details of the K^0p spectrum, we first examine which conditions are better to reach the "Θ^+" energy region and to search for its peak. To this end, we calculate the K^0p invariant mass of the $K^+d \to K^0pp$ reaction, assuming that the nucleon Fermi motion is zero and that the reaction takes place only in the impulse scattering process. In this case, one proton is produced from a zero-momentum neutron in the initial state of the $K^+n \to K^0p$ reaction, while the other proton comes out just as a spectator. Then, we can calculate the K^0p invariant mass in two ways: combining K^0 with the produced proton in the impulse scattering process, and K^0 with the spectator proton. Namely, in terms of the formulation in Sect. 2.1, the former (latter) case means that the produced proton is the "first" ("second") proton while the spectator is the "second" ("first") proton.

The K^0p invariant mass of these two methods is plotted in Fig. 2 in terms of the square boxes (former) and curves (latter), respectively. We note that, in general, the possible K^0p invariant mass discussed here is slightly smeared compared with those in Fig. 2 due to the Fermi motion of the nucleons inside a deuteron. As one can see, on the one hand, the square boxes in Fig. 2 reach around the "Θ^+" energy region $\sim$ 1.52 GeV with the initial kaon momentum $k_{\rm lab} \approx 0.40$ GeV/c. This means that one can investigate the "Θ^+" energy region directly in the impulse scattering process with the initial kaon momentum $k_{\rm lab} \approx 0.40$ GeV/c and with the backward "second" proton. On the other hand, the curves in Fig. 2 suggest that even with higher kaon momenta one can reach the "Θ^+" energy region by observing the forward "second" proton. In this case, although the impulse scattering process cannot produce the "Θ^+", double-step scattering can do it, where the intermediate kaon may lead to the formation of the "Θ^+", being combined with the "first" proton.

Therefore, the present study is two-fold. Firstly, we check whether a possible "Θ^+" signal will appear in the impulse scattering process with lower kaon momenta $k_{\rm lab} \approx 0.40$ GeV/c. In fact, Ref. [47] already carried this out. Thus, in the first part of the present work, we extend Ref. [47] and perform a more detailed analysis of the study. Secondly, we investigate whether the double-step scattering contribution with higher kaon momenta $k_{\rm lab} \sim 1$ GeV/c can generate the "Θ^+" in the $K^+d \to K^0pp$ reaction.

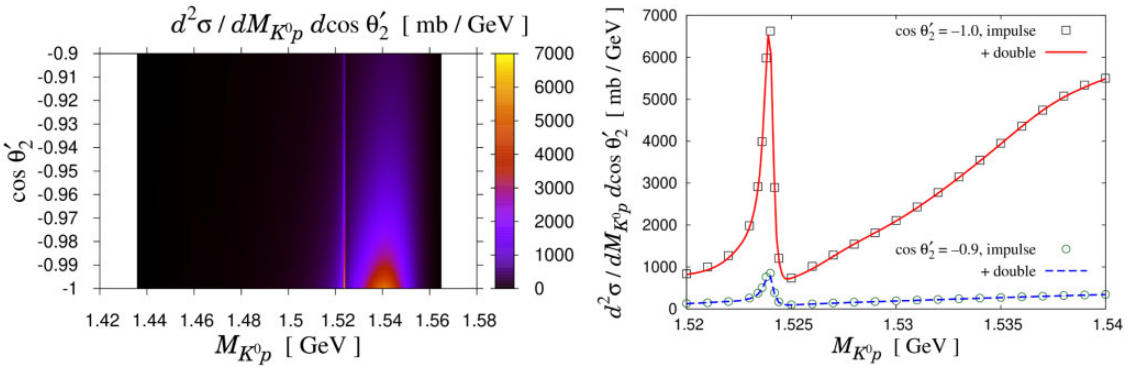

Fig. 3. Results for the differential cross section of the $K^+d \to K^0pp$ reaction in the impulse scattering process (left) and a comparison of the differential cross section with and without the double-step processes at $\cos\theta_2' = -1.0$ and -0.9 (right). The initial kaon momentum is fixed as $k_{\rm lab} = 0.45$ GeV/c. The "Θ^+" with $J^P = 1/2^+$ is taken into account.

3.2. Lower kaon momentum

Let us first consider the case of lower kaon momenta. In this case, we expect that the impulse scattering process dominates the $K^+d \to K^0pp$ reaction. Indeed, we will see that this is the case at lower kaon momenta, since the double-step processes give only a few % contribution to the differential cross section. In the following discussions for lower momentum we examine the impulse scattering process only, unless explicitly mentioned. This allows one to check how the results of the cross section for the $K^+d \to K^0pp$ reaction are affected when the "Θ^+" is taken into account.

In order to see how the "Θ^+" influences the cross section, we show in Fig. 3 the results for the differential cross section $d^2\sigma/dM_{K^0p}\cos\theta_2'$ with the initial kaon momentum $k_{\rm lab} = 0.45$ GeV/c. The "Θ^+" with $J^P = 1/2^+$ is taken into account. Here we show only the region $\cos\theta_2' \leq -0.9$ because there is no significant structure in the region $\cos\theta_2' > 0.9$. We find two structures in the contour plot of Fig. 3: a sharp peak at $M_{K^0p} = 1.524$ GeV as a "Θ^+" signal and a broad bump at $M_{K^0p} = 1.54$ GeV and $\cos\theta_2' = -1$ corresponding to the square boxes in Fig. 2, arising from the kinematical effects. The Fermi motion of the bound neutron due to the deuteron wave function, on the one hand, makes the peak at $(M_{K^0p}, \cos\theta_2') = (1.54\ {\rm GeV}, -1)$ broad. On the other hand, thanks to the same Fermi motion of the bound neutron, we can reach the "Θ^+" energy in the impulse scattering process even when the initial kaon momentum does not exactly match the kaon momentum that generates the two-body CM energy 1.524 GeV with a free nucleon at rest, i.e., the kaon momentum $k_{\rm lab} \approx 0.40$ GeV/c. Therefore, we can observe the "Θ^+" signal with $k_{\rm lab} = 0.45$ GeV/c as in the left panel of Fig. 3.

To confirm that the impulse scattering process dominates the $K^+d \to K^0pp$ reaction in the lower kaon momentum case, we compare in the right panel of Fig. 3 the differential cross section $d^2\sigma/dM_{K^0p}\cos\theta_2'$ only with the impulse scattering (points) and that with the double-step processes (lines). The initial kaon momentum is $k_{\rm lab} = 0.45$ GeV/c, the spin/parity of the "Θ^+" is $J^P = 1/2^+$, and the scattering angles $\cos\theta_2' = -1.0$ and -0.9 are considered. From the right panel of Fig. 3 we can see that the contributions from the double-step processes are indeed negligible in the lower kaon momentum case. Indeed, the double-step processes give only a few % contribution to the differential cross section. The same behavior is observed at other angles $\cos\theta_2'$ and other (but lower) kaon momenta. Therefore, we can safely concentrate on the impulse scattering process in this subsection.

We discuss the same reaction with the Dalitz plot $d^2\sigma/dM_{K^0p(1)}dM_{K^0p(2)}$. In Fig. 4 we show the Dalitz plot with $k_{\rm lab} = 0.45$ GeV/c and the "Θ^+" with spin and parity $J^P = 1/2^+$. Broad structures

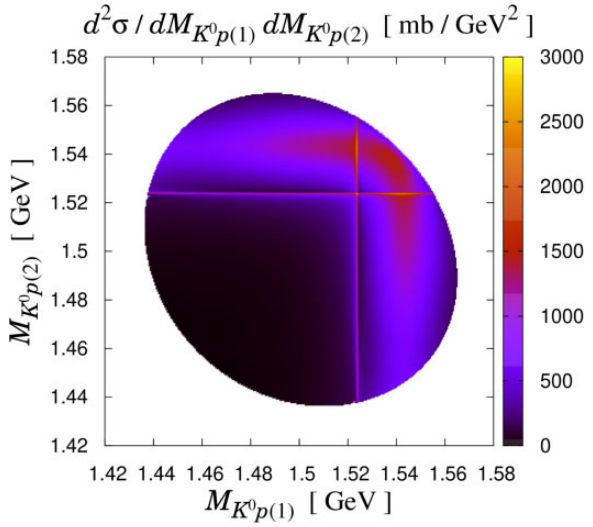

Fig. 4. Dalitz plot of the $K^+d \to K^0pp$ reaction in the impulse scattering process. The initial kaon momentum is fixed as $k_{\rm lab} = 0.45$ GeV/c. The "Θ^+" with $J^P = 1/2^+$ is taken into account.

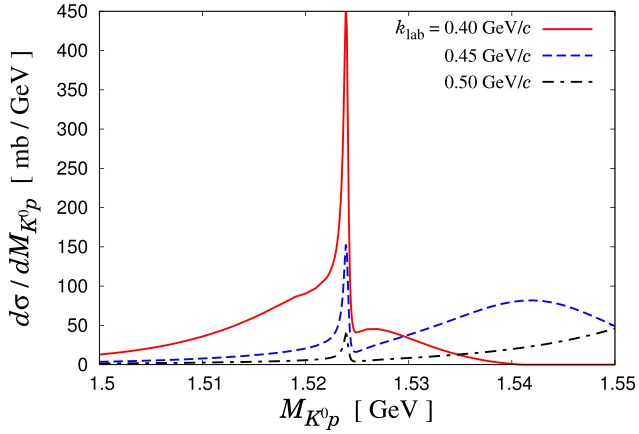

Fig. 5. K^0p invariant mass spectrum of the $K^+d \to K^0pp$ reaction with initial kaon momenta $k_{\rm lab} = 0.40$ GeV/c, 0.45 GeV/c, and 0.50 GeV/c in the impulse scattering process. The integral range of the scattering angle is $-1 < \cos\theta_2' < -0.8$. The "$\Theta^+$" with $J^P = 1/2^+$ is taken into account.

around $M_{K^0p(1)} \sim 1.54$ in the vertical direction and $M_{K^0p(2)} \sim 1.54$ in the horizontal direction originate from the kinematical effects, which correspond to the square boxes in Fig. 2. In addition, sharp structures at $M_{K^0p(1)} = 1.524$ in the vertical direction and $M_{K^0p(2)} = 1.524$ in the horizontal direction indicate the "Θ^+" signal.

In Fig. 5 we plot the K^0p invariant mass spectra of the $K^+d \to K^0pp$ reaction with three initial kaon momenta $k_{\rm lab} = 0.40$ GeV/c, 0.45 GeV/c, and 0.50 GeV/c. Here we take into account the "Θ^+" contribution with $J^P = 1/2^+$, and we integrate with respect to the scattering angle in the range $-1 < \cos\theta_2' < -0.8$. As one can see from Fig. 5, on the one hand, the broad-peak structure, which corresponds to impulse scattering of the initial kaon and almost on-shell bound neutron, moves upward as $k_{\rm lab}$ increases, as expected from the square boxes in Fig. 2. On the other hand, the "Θ^+" signal stays at 1.524 GeV with different values of $k_{\rm lab}$. Among the three values of the kaon momenta, $k_{\rm lab} = 0.40$ GeV/c yields the highest peak at $M_{K^0p} = 1.524$ GeV for the "Θ^+" signal on top of the broad peak. This is a consequence of the momentum matching in Fig. 2.

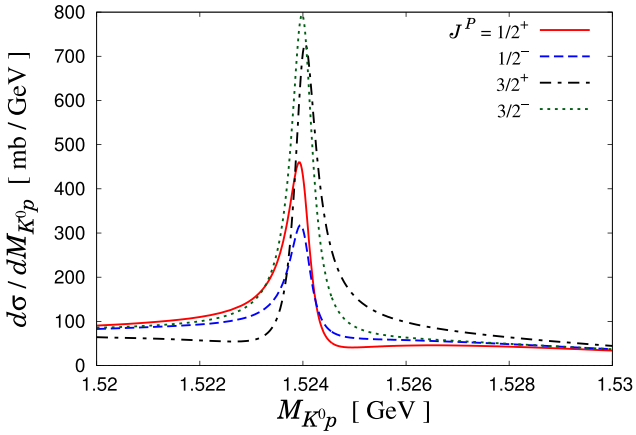

Fig. 6. K^0p invariant mass spectrum of the $K^+d \to K^0pp$ reaction in the impulse scattering process with the "Θ^+" spin/parity $J^P = 1/2^\pm$ and $3/2^\pm$. The initial kaon momentum is fixed as $k_{\rm lab} = 0.40$ GeV/c. The integral range of the scattering angle is $-1 < \cos\theta_2' < -0.8$.

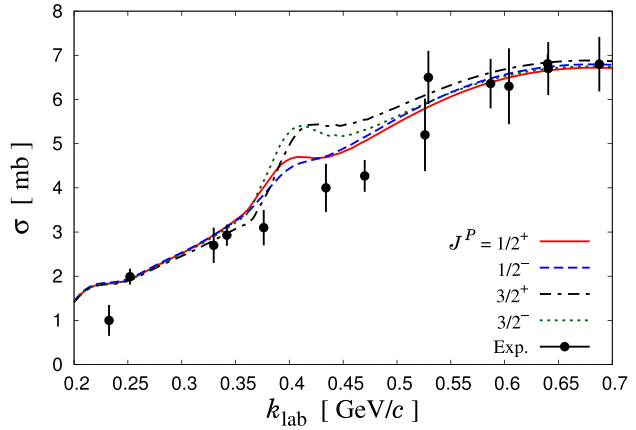

Fig. 7. Total cross section of the $K^+d \to K^0pp$ reaction as a function of the initial kaon momentum in the laboratory frame $k_{\rm lab}$. We take into account only the impulse scattering. The experimental data are taken from Refs. [61–64].

We then examine other spin/parity combinations of the "Θ^+" pentaquark: $J^P = 1/2^-$, $3/2^+$, and $3/2^-$. In Fig. 6 we show the K^0p invariant mass spectrum of the $K^+d \to K^0pp$ reaction with the initial kaon momentum $k_{\rm lab} = 0.40$ GeV/c and with the "Θ^+" of $J^P = 1/2^\pm$ and $3/2^\pm$. The integral range of the scattering angle is $-1 < \cos\theta_2' < -0.8$. Figure 6 indicates that the peak heights for the "Θ^+" signal in different quantum numbers are similar to each other. These peaks generate the "Θ^+" production cross section $\sim$ several hundred μb to 1 mb with $k_{\rm lab} \approx 0.40$ GeV/c.

Finally we calculate the total cross section of the $K^+d \to K^0pp$ reaction with the "Θ^+" contribution of spin/parity $J^P = 1/2^\pm$ and $3/2^\pm$. The result is shown in Fig. 7 together with the old experimental data on $K^+d \to K^0pp$ scattering [61–64]. Note that similar results were already obtained in Ref. [47], in which, however, the width of the "Θ^+" was taken to be 1–20 MeV. As shown in Fig. 7, even if the decay width of the "Θ^+" is as small as $\Gamma_\Theta = 0.5$ MeV, which is approximately 2–40 times smaller than those in Ref. [47], one can observe a bump structure around the initial kaon momentum in the laboratory frame $k_{\rm lab} = 0.4$ GeV/c. The height of the bump gives indeed a few hundred μb to 1 mb. While the old experiments lack data in the vicinity of $k_{\rm lab} \approx 0.4$ GeV/c, new experiments

at the J-PARC, if performed exclusively near this value of the initial kaon momentum in the near future, will be able to assess the existence of the "Θ^+", because the size of the bump structure (a few hundred μb to 1 mb) is still strong enough to be seen. In order to check a bump structure in the total cross section in Fig. 7, the required resolution of the initial kaon momentum is about several tens of MeV/c, while one can observe the "Θ^+" peak, if it exists, in the K^0p invariant mass spectrum as in Fig. 6 with the resolution of the K^0p invariant mass $\sim$ 1 MeV.

3.3. Higher kaon momentum

We now focus on the case of higher kaon momenta. To reach the "Θ^+" energy region with higher kaon momenta, we need to consider the double-step scattering process where the initial K^+ produces a proton from the deuteron in the first collision, losing some of its momentum. Then, it interacts with the other nucleon in the second collision. In this process, the first collision corresponds to the $K^+p \to K^+p$ or $K^+n \to K^0p$ reaction of the forward proton emission. In this sense, the initial kaon momentum should be chosen such that the forward proton emission efficiently takes place in the first collision. In other words, we require a specific initial kaon momentum in such a way that the $K^+p \to K^+p$ and $K^+n \to K^0p$ cross sections with the forward proton emission should be large. In fact, this strategy was employed to search for a $\bar{K}NN$ quasi-bound state in the $K^-{}^3\mathrm{He} \to \Lambda pn$ reaction in the J-PARC E15 experiment [65,66]. In the J-PARC E15 experiment, to generate a $\bar{K}NN$ quasi-bound state, they planned to prepare a slow antikaon and two of the three bound nucleons in ^{3}He by using the $K^-n \to K^-n$ or $K^-p \to \bar{K}^0n$ reaction with the fast forward neutron emission as the first collision, which eventually leads to the $\bar{K}NN$ quasi-bound state (see also the theoretical calculation of the $K^-{}^3\mathrm{He} \to \Lambda pn$ reaction in Ref. [67]). To prepare a slow antikaon and fast forward neutron emission as much as possible, the initial K^- momentum $k_{\mathrm{lab}} = 1.0$ GeV/c was selected in Refs. [65,66].

As shown in the top panels of Fig. 8 for the differential cross sections of the $\bar{K}N \to \bar{K}N$ reaction as functions of the initial antikaon momentum k_{lab} and antikaon scattering angle θ_K, the $\bar{K}N \to \bar{K}N$ differential cross section indeed reveals a peak structure at $k_{\mathrm{lab}} \approx 1$ GeV/c and $\cos_K \approx -1$, which is essential to obtain a slow antikaon with the forward neutron emission.

When it comes to the $KN \to KN$ case, the bottom panels of Fig. 8 illustrate the $K^+p \to K^+p$ and $K^+n \to K^0p$ reaction cross sections, which indicates that $k_{\mathrm{lab}} = 0.8$–0.9 GeV/c are the best values for the present study of the $K^+d \to K^0pp$ reaction. With these kaon momenta, we obtain the largest cross sections of the $K^+n \to K^0p$ and $K^+p \to K^+p$ reactions at $\cos\theta_K \approx -1$, which corresponds to the forward proton emission. Thus, we fix the initial kaon momentum to be $k_{\mathrm{lab}} = 0.85$ GeV/c and compute the K^0p invariant mass spectrum of the $K^+d \to K^0pp$ reaction. Note that we take into account here both the double-step scattering process and the impulse scattering one.

In Fig. 9, we show the results of the differential cross section in the "Θ^+" energy region including the "Θ^+" with $J^P = 1/2^+$. Figure 9 exhibits three structures: a band at $\cos\theta_2' \gtrsim 0.5$, a thin line at $M_{K^0p} = 1.524$ GeV, and a sharp peak at $(M_{K^0p}, \cos\theta_2') = (1.524\ \mathrm{GeV}, -1)$. The first band structure corresponds to the line in Fig. 2 and originates from the impulse scattering contribution. Note, however, that it was parametrized in terms of the invariant mass of K^0 and spectator proton. The second one, the line structure, represents a signal of the "Θ^+". The impulse scattering process cannot generate the line structure because in such a case a highly off-shell neutron is required. Therefore, we can conclude that this line structure is given by the double-step scattering process. The third one, which corresponds to the sharp peak around 1.524 GeV and $\cos\theta_2' = -1$, arises from the "Θ^+" production in the impulse scattering process with a highly off-shell bound nucleon.

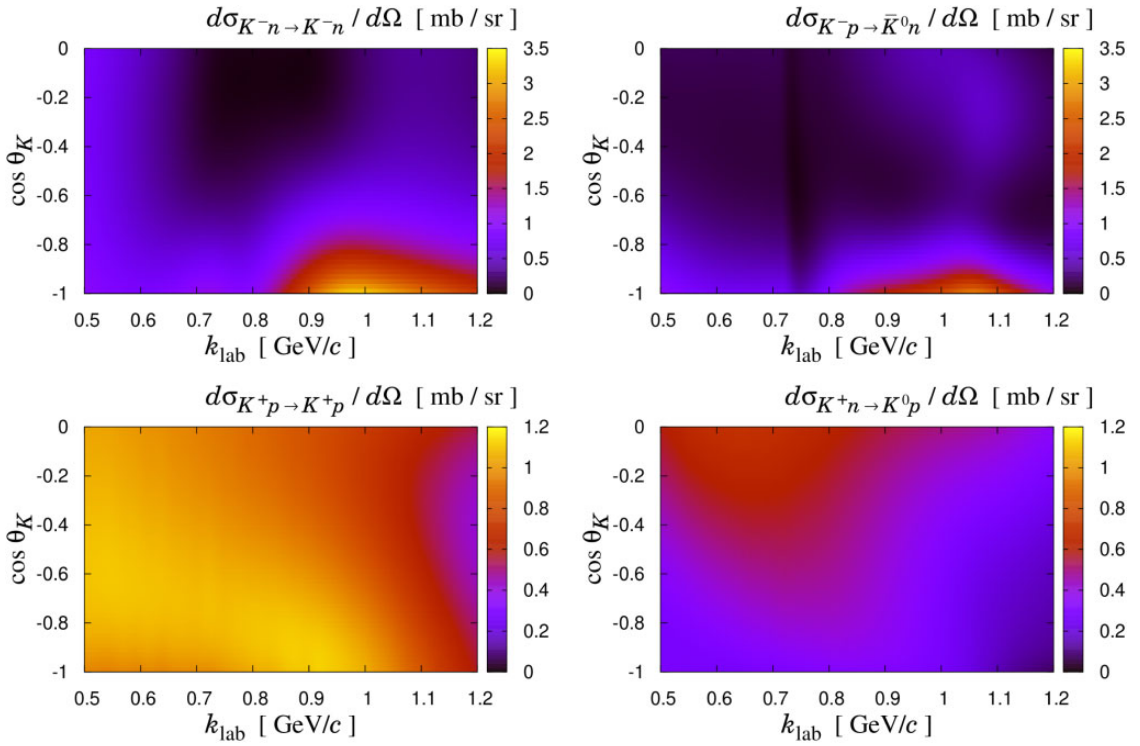

Fig. 8. Differential cross sections of the $K^-n \to K^-n$ (top left), $K^-p \to \bar{K}^0n$ (top right), $K^+p \to K^+p$ (bottom left), and $K^+n \to K^0p$ (bottom right) reactions. The $\bar{K}N \to \bar{K}N$ cross sections are taken from a dynamical coupled-channels model, and the $KN \to KN$ cross sections are calculated with the SAID amplitudes [59].

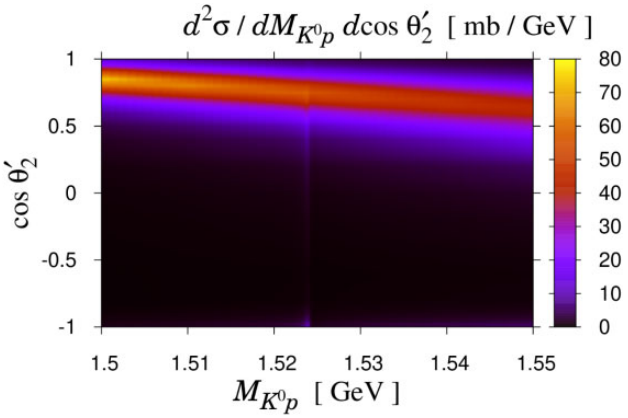

Fig. 9. Differential cross section of the $K^+d \to K^0pp$ reaction in the impulse plus double scattering processes. The initial kaon momentum is fixed as $k_{\rm lab} = 0.85$ GeV/c. The "Θ^+" with $J^P = 1/2^+$ is taken into account.

This contribution, however, depends on the tail of the deuteron wave function in momentum space and thus contains large theoretical uncertainty. Therefore, we do not regard this third sharp-peak structure at $(M_{K^0p}, \cos\theta_2') = (1.524\ \text{GeV}, -1)$ as an important one.

As in the lower kaon momentum case, we can discuss the same reaction with the Dalitz plot $d^2\sigma/dM_{K^0p(1)}dM_{K^0p(2)}$. In Fig. 10 we show the Dalitz plot with $k_{\rm lab} = 0.85$ GeV/c and the "Θ^+" spin/parity $J^P = 1/2^+$. We can hardly distinguish the "Θ^+" signal around $M_{K^0p(1)} = 1.524$ in the vertical direction and $M_{K^0p(2)} = 1.524$ in the horizontal direction because the impulse scattering process dominates the reaction as a whole. Nevertheless, if we enlarge the Dalitz plot, we can

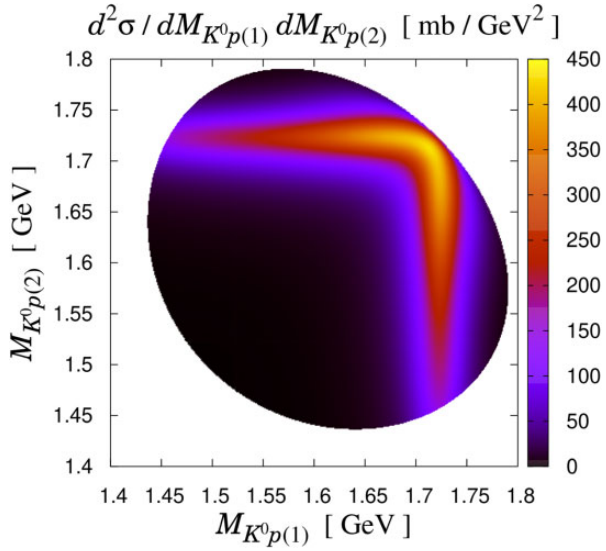

Fig. 10. Dalitz plot of the $K^+d \to K^0pp$ reaction in the impulse plus double scattering processes. The initial kaon momentum is fixed as $k_{\rm lab} = 0.85$ GeV/c. The "Θ^+" with $J^P = 1/2^+$ is taken into account.

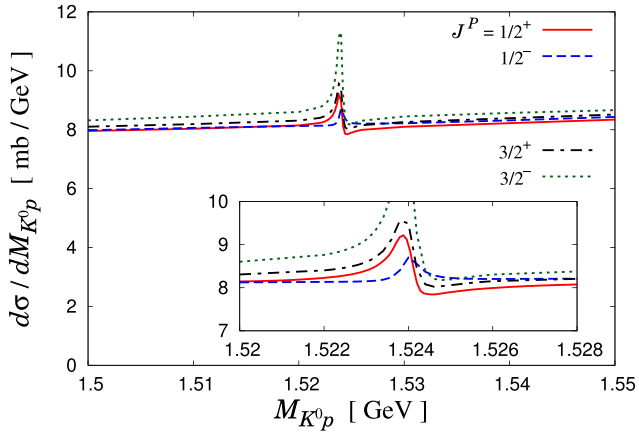

Fig. 11. K^0p invariant mass spectrum of the $K^+d \to K^0pp$ reaction in the impulse and double-step scattering processes with the "Θ^+" spin/parity $J^P = 1/2^\pm$ and $3/2^\pm$. The initial kaon momentum is fixed to be $k_{\rm lab} = 0.85$ GeV/c. The integral range of the scattering angle is given as $0 < \cos\theta_2' < 1$. The inset represents an enlarged figure.

observe small sharp structures at $M_{K^0p(1)} = 1.524$ in the vertical direction and $M_{K^0p(2)} = 1.524$ in the horizontal direction as the "Θ^+" signal.

Now the very important task is to answer how significant the signal of the "Θ^+" in the double-step scattering process, i.e., the thin line structure in Fig. 9, is compared to the impulse scattering contribution parametrized in terms of the invariant mass of K^0 and spectator proton band in Fig. 9. To do that, we integrate the differential cross section of Fig. 9 with the integral range $0 < \cos\theta_2' < 1$, which results in the K^0p invariant mass spectrum in Fig. 11. Here we have introduced the "Θ^+" contribution of spin/parity $J^P = 1/2^\pm$ and $3/2^\pm$. As shown in Fig. 11, with every spin/parity of the "Θ^+", a small "Θ^+" signal exists on a smooth background. The smooth background out of the "Θ^+" energy comes from the broad band at $\cos\theta_2' \gtrsim 0.5$ in Fig. 9, so we can see that the background originates from the impulse scattering contribution. This dominates the cross section

(i.e., the integral of the mass spectrum) of the reaction. Nevertheless, the small "Θ^+" signal is not invisible owing to the double-step processes. By calculating the excess area of the spectrum in Fig. 11 on top of the background from the impulse scattering contribution, we find that the "Θ^+" production cross section turns out to be about 0.9 μb, 0.4 μb, 1 μb, and 3 μb for the spin/parity of the "Θ^+" $J^P = 1/2^+$, $J^P = 1/2^-$, $J^P = 3/2^+$, and $J^P = 3/2^-$, respectively. Therefore, we expect that in the $K^+d \to K^0pp$ reaction with higher kaon momenta $k_{\rm lab} \approx 0.85$ GeV/c a measurement of the production cross section $\lesssim 1$ μb is required to save the "Θ^+" pentaquark. One can experimentally assess the existence of such a narrow peak in the K^0p spectrum with the resolution of the K^0p invariant mass ~ 1 MeV.

4. Summary and outlook

In the present work, we have investigated the $K^+d \to K^0pp$ reaction as a feasibility study to suggest the kinematical conditions for the most probable range of the initial kaon momentum and to assess the existence of the "Θ^+" pentaquark in this reaction. We consider two different dynamical processes for the $K^+d \to K^0pp$ reaction, i.e., the single-step or impulse scattering process and the double-step scattering process. While the first was already considered in a previous study, the latter was ignored. In the present work, we took into account both the processes and scrutinized the kinematical conditions relevant to each process and their relevances in the production of the "Θ^+" pentaquark. We showed explicitly that, to produce the "Θ^+", the impulse scattering process is dominant over the double-step scattering process in lower-momentum regions ($k_{\rm lab} \approx 0.40$ GeV/c), whereas the double-step one overtakes the impulse one in higher-momentum regions ($k_{\rm lab} \approx 0.85$ GeV/c). We found that the strength of the bump structure corresponding to the "Θ^+" is about a few hundred μb to 1 mb in the lower-momentum region, while it is about 1 μb in the higher-momentum region.

The K^+ beam has a unique feature in investigating the existence of the "Θ^+", compared with almost all experiments done previously. This tentative pentaquark state "Θ^+" is strongly coupled to either K^+n or K^0p. This implies that the charged K^+ beam provides a chance to produce the "Θ^+" by direct formation. Thus, it is not necessary to resort to any complicated methods of experimental analysis to observe the "Θ^+", if it exists. In this sense, J-PARC is the best place to perform the ultimate experiments with the K^+ beam to put a final period to the matter of the "Θ^+" existence. It is physically worthwhile to carry out such experiments in the future. If the experiments at J-PARC find that "Θ^+" does not exist, it will bring any debate on the existence of the "Θ^+" to an end. However, if the experiments yield any evidence for its existence, it will reignite interest in the physics of light pentaquarks.

Acknowledgements

The authors want to express their gratitude to M. Oka and K. Tanida for useful discussions. H.-Ch.K. is also grateful to M. V. Polyakov and Gh.-S. Yang for valuable discussions and comments. He is also very grateful to the members of the Advanced Science Research Center (ASRC), Japan Atomic Energy Agency (JAEA), where part of the work was carried out, for the hospitality and support. H.-Ch.K. is supported by the Basic Science Research Program through the National Research Foundation of Korea funded by the Ministry of Education, Science and Technology (2018R1A2B2001752 and 2018R1A5A1025563). A.H. is supported in part by JSPS KAKENHI No. JP17K05441 (C) and Grants-in-Aid for Scientific Research on Innovative Areas (No. 18H05407).

Funding

Open Access funding: SCOAP[3].

References

[1] R. Aaij et al. [LHCb Collaboration], Phys. Rev. Lett. **115**, 072001 (2015).
[2] R. Aaij et al. [LHCb Collaboration], Phys. Rev. Lett. **117**, 082002 (2016).
[3] R. Aaij et al. [LHCb Collaboration], Phys. Rev. Lett. **117**, 082003 (2016); **117**, 109902 (2016); **118**, 119901 (2017) [errata].
[4] R. Aaij et al. [LHCb Collaboration], Phys. Rev. Lett. **122**, 222001 (2019).
[5] R. Aaij et al. [LHCb Collaboration], Phys. Rev. Lett. **118**, 182001 (2017).
[6] J. Yelton et al. [Belle Collaboration], Phys. Rev. D **97**, 051102 (2018).
[7] H.-Ch. Kim, M. V. Polyakov, and M. Praszalowicz, Phys. Rev. D **96**, 014009 (2017); **96**, 039902 (2017) [erratum].
[8] H.-Ch. Kim, M. V. Polyakov, M. Praszalowicz, and G. S. Yang, Phys. Rev. D **96**, 094021 (2017); **97**, 039901 (2018) [erratum].
[9] C. S. An and H. Chen, Phys. Rev. D **96**, 034012 (2017).
[10] Z. G. Wang and J. X. Zhang, Eur. Phys. J. C **78**, 503 (2018).
[11] D. Diakonov, V. Petrov, and M. V. Polyakov, Z. Phys. A **359**, 305 (1997).
[12] T. Nakano et al. [LEPS Collaboration], Phys. Rev. Lett. **91**, 012002 (2003).
[13] M. Battaglieri et al. [CLAS Collaboration], Phys. Rev. Lett. **96**, 042001 (2006).
[14] B. McKinnon et al. [CLAS Collaboration], Phys. Rev. Lett. **96**, 212001 (2006).
[15] R. De Vita et al. [CLAS Collaboration], Phys. Rev. D **74**, 032001 (2006).
[16] K. Miwa et al. [KEK-PS E522 Collaboration], Phys. Lett. B **635**, 72 (2006).
[17] K. Shirotori et al., Phys. Rev. Lett. **109**, 132002 (2012).
[18] M. Moritsu et al. [J-PARC E19 Collaboration], Phys. Rev. C **90**, 035205 (2014).
[19] C. P. Shen et al. [Belle Collaboration], Phys. Rev. D **93**, 112017 (2016).
[20] T. Nakano et al. [LEPS Collaboration], Phys. Rev. C **79**, 025210 (2009).
[21] M. Niiyama [LEPS and LEPS II Collaborations], Nucl. Phys. A **914**, 543 (2013).
[22] V. V. Barmin et al. [DIANA Collaboration], Phys. Rev. C **89**, 045204 (2014).
[23] V. V. Barmin et al. [DIANA Collaboration], arXiv:1507.06001 [hep-ex] [Search INSPIRE].
[24] M. J. Amaryan et al., Phys. Rev. C **85**, 035209 (2012).
[25] A. E. Asratyan and V. A. Matveev, arXiv:1608.08523 [hep-ex] [Search INSPIRE].
[26] V. Kuznetsov et al. [GRAAL Collaboration], Phys. Lett. B **647**, 23 (2007).
[27] F. Miyahara et al., Prog. Theor. Phys. Suppl. **168**, 90 (2007).
[28] V. Kuznetsov, M. V. Polyakov, T. Boiko, J. Jang, A. Kim, W. Kim, H. S. Lee, A. Ni and G. S. Yang, Acta Phys. Polon. B **39**, 1949 (2008).
[29] I. Jaegle et al. [CBELSA/TAPS Collaboration], Phys. Rev. Lett. **100**, 252002 (2008).
[30] I. Jaegle et al. [CBELSA/TAPS Collaboration], Eur. Phys. J. A **47**, 89 (2011).
[31] D. Werthmüller et al. [A2 Collaboration], Phys. Rev. Lett. **111**, 232001 (2013).
[32] L. Witthauer et al. [A2 Collaboration], Eur. Phys. J. A **49**, 154 (2013).
[33] D. Werthmüller et al. [A2 Collaboration], Phys. Rev. C **90**, 015205 (2014).
[34] E. F. McNicoll et al. [Crystal Ball at MAMI Collaboration], Phys. Rev. C **82**, 035208 (2010); **84**, 029901 (2011) [erratum].
[35] L. Witthauer et al. [A2 Collaboration], Phys. Rev. Lett. **117**, 132502 (2016).
[36] V. Metag and M. Nanova [CBELSA/TAPS Collaboration], EPJ Web Conf. **199**, 02008 (2019).
[37] M. V. Polyakov and A. Rathke, Eur. Phys. J. A **18**, 691 (2003).
[38] H.-Ch. Kim, M. Polyakov, M. Praszalowicz, G. S. Yang, and K. Goeke, Phys. Rev. D **71**, 094023 (2005).
[39] G. S. Yang and H.-Ch. Kim, Prog. Theor. Exp. Phys. **2019**, 093D01 (2019).
[40] A. Martinez Torres and E. Oset, Phys. Rev. Lett. **105**, 092001 (2010).
[41] A. Martinez Torres and E. Oset, Phys. Rev. C **81**, 055202 (2010).
[42] V. V. Barmin et al. [DIANA Collaboration], Phys. Atom. Nucl. **66**, 1715 (2003) [Yad. Fiz. **66**, 1763 (2003)].
[43] V. V. Barmin et al. [DIANA Collaboration], Phys. Atom. Nucl. **70**, 35 (2007).
[44] V. V. Barmin et al. [DIANA Collaboration], Phys. Atom. Nucl. **73**, 1168 (2010).
[45] A. Sibirtsev, J. Haidenbauer, S. Krewald, and U. G. Meissner, Eur. Phys. J. A **23**, 491 (2005).
[46] A. Gal and E. Friedman, Phys. Rev. C **73**, 015208 (2006).
[47] A. Sibirtsev, J. Haidenbauer, S. Krewald, and U. G. Meissner, Phys. Lett. B **599**, 230 (2004).

[48] E949 Pentaquark studies (available at: https://www.phy.bnl.gov/e949/analysis/pentaquark/, date last accessed May 17, 2020).
[49] T. Nakano et al., *Letter of intent for study of exotic hadrons with $S = +1$ and rare decay $K^+ \to \pi^+ \nu\bar{\nu}$ with low-momentum kaon beam at J-PARC* (2006) (available at: http://j-parc.jp/researcher/Hadron/en/pac_0606/pdf/p09-Nakano.pdf, date last accessed May 17, 2020). First PAC meeting at J-PARC.
[50] K. Tanida and M. Yosoi, *Letter of intent for search for Θ^+ hypernuclei using (K^+, p) reaction* (2007) (available at: http://j-parc.jp/researcher/Hadron/en/pac_0801/pdf/LOI_Tanida_pentahyper.pdf, date last accessed May 17, 2020). Fourth PAC meeting at J-PARC.
[51] D. Jido, E. Oset, and T. Sekihara, Eur. Phys. J. A **42**, 257 (2009).
[52] D. Jido, E. Oset, and T. Sekihara, Eur. Phys. J. A **47**, 42 (2011).
[53] D. Jido, E. Oset, and T. Sekihara, Eur. Phys. J. A **49**, 95 (2013).
[54] J. Yamagata-Sekihara, T. Sekihara, and D. Jido, Prog. Theor. Exp. Phys. **2013**, 043D02 (2013).
[55] W. R. Gibbs, Phys. Rev. C **70**, 045208 (2004).
[56] M. Lacombe, B. Loiseau, R. Vinh Mau, J. Cote, P. Pires, and R. de Tourreil, Phys. Lett. B **101**, 139 (1981).
[57] R. Machleidt, Phys. Rev. C **63**, 024001 (2001).
[58] H. Kamano and T.-S. H. Lee, Phys. Rev. C **94**, 065205 (2016).
[59] INS Data Analysis Center, *INS DAC services* (Institute for Nuclear Studies, Ashburn, VA) (available at: http://gwdac.phys.gwu.edu, date last accessed May 17, 2020). SAID Program.
[60] G. S. Yang and H.-Ch. Kim, Prog. Theor. Exp. Phys. **2013**, 013D01 (2013).
[61] W. Slater, D. H. Stork, H. K. Ticho, W. Lee, W. Chinowsky, G. Goldhaber, S. Goldhaber, and T. O'Halloran, Phys. Rev. Lett. **7**, 378 (1961).
[62] G. Giacomelli et al., Nucl. Phys. B **37**, 577 (1972).
[63] C. J. S. Damerell et al., Nucl. Phys. B **94**, 374 (1975).
[64] R. G. Glasser, G. A. Snow, D. Trevvett, R. A. Burnstein, C. Fu, R. Petri, G. Rosenblatt, and H. A. Rubin, Phys. Rev. D **15**, 1200 (1977).
[65] Y. Sada et al. [J-PARC E15 Collaboration], Prog. Theor. Exp. Phys. **2016**, 051D01 (2016).
[66] S. Ajimura et al. [J-PARC E15 Collaboration], Phys. Lett. B **789**, 620 (2019).
[67] T. Sekihara, E. Oset, and A. Ramos, Prog. Theor. Exp. Phys. **2016**, 123D03 (2016).
[68] H. Kamano, S. X. Nakamura, T.-S. H. Lee, and T. Sato, Phys. Rev. C **90**, 065204 (2014).